

Nitrogen fixation by rotational gliding arc plasma at surrounding conditions

Avik Denra^a, Shirjana Saud^{a,*}, Duc Ba Nguyen^{b,c}, Quang Thang Trinh^d, Tuan-Khoa Nguyen^d, Hongjie An^d, Nam-Trung Nguyen^d, Sosiawati Teke^a, Young Sun Mok^{a,*}

^a Department of Chemical Engineering, Jeju National University, Jeju, 63243, Republic of Korea

^b Institute of Theoretical and Applied Research, Duy Tan University, Hanoi, 100000, Viet Nam

^c Institute of Research and Development, Duy Tan University, Danang, 550000, Viet Nam

^d Queensland Micro and Nanotechnology Centre, Griffith University, Nathan, Queensland, 4111, Australia

ARTICLE INFO

Handling Editor: Jin-Kuk Kim

Keywords:

Nitrogen fixation
Rotational gliding arc
NO_x generation
Oxygen content
Water content
HNO₃ formation
Air plasma

ABSTRACT

Nitrogen fixation (NF) was investigated in a rotational gliding arc plasma based on various energy inputs, flow rates, and N₂:O₂ ratios under atmospheric conditions. For practical application, the effect of water content in the feed, self-heating during plasma discharge, prolonged operation, and comparison between plasma and thermal process for N₂ oxidation were also conducted. The comparison results reveal that NF by the gliding arc plasma is superior to the thermal process in terms of NO_x yield and energy consumption at low temperatures and atmospheric pressure. Herein, energy input and flow rate are two controlled factors that significantly influence NO_x production rate. Simultaneously, O₂ content played a crucial role in determining NO_x yield, selectivity of NO/NO₂, and energy consumption. Observations during plasma discharge indicated an initial rise in gas and reactor body temperatures, coinciding with decrease in total NO_x formation. Moreover, the presence of water had a negative effect on NO_x yield. Accordingly, the optimized conditions for NF by gliding arc plasma for NO_x formation was identified at a N₂ to O₂ ratio of 3:2 without water vapor in the feed gas. Furthermore, a 14-h continuous operational test validated the robustness of our reactor configuration, affirming its long-term viability. The study concludes by performing oxidation of the NO_x gas followed by dissolution in water, successfully generating nitric acid. These findings underscore the potential of gliding arc plasma for efficient NF processes, offering insights into optimal operational conditions and downstream applications for nitric acid generation.

1. Introduction

Nitrogen fixation (NF) remains one of the most extensively investigated processes owing to its crucial significance in agricultural science (Cherkasov et al., 2015; Roy et al., 2023). In spite of being abundantly available, atmospheric Nitrogen (N₂) is chemically inert due to the presence of the strong triple bond (Wang et al., 2023). Thus, NF is necessary to convert the atmospheric N₂ into its other forms (such as ammonia or nitrate) that can be used by plants and animals. The production of nitrogen fertilizers in industries is essential to meet the recent demand for higher crop yield (Tsonev, I. et al., 2023). Indeed, the most widely used process for industrial NF is the Haber-Bosch process which utilizes N₂ and hydrogen (H₂) to produce NH₃ (Humphreys et al., 2021;

Liu et al., 2021). However, the Haber-Bosch process typically operates under high pressure and temperature conditions (150–200 Bar; 400–500 °C) along with the consumption of a large amount of energy (Foster et al., 2018; Steinberger-Wilckens and Sampson, 2019; Wu et al., 2021). Typically, up to 3% of the entire worldwide energy sector is used every year for the Haber-Bosch process. (Cherkasov et al., 2015; Kelly and Bogaerts, 2021; Wang et al., 2017, 2022). Furthermore, the primary energy feed is obtained from gas power plants and H₂ being sourced from the combustion of natural gas which leads to tons of CO₂ emission. (Wang et al., 2017; Winter and Chen, 2021). These drawbacks of the commercial process demand the improvement of other ways of NF methods that can be more efficient and easier in practical applications.

Among NF methods, plasma technology is an alternative approach

* Corresponding author.

** Corresponding author.

E-mail addresses: saudshirju@gmail.com (S. Saud), smokie@jejunu.ac.kr (Y.S. Mok).

<https://doi.org/10.1016/j.jclepro.2024.140618>

Received 13 October 2023; Received in revised form 31 December 2023; Accepted 4 January 2024

Available online 10 January 2024

0959-6526/© 2024 Elsevier Ltd. All rights reserved.

for N_2 conversion using electrical energy for the generation of reactive nitrogen species. (Kelly et al., 2022; Patil et al., 2015). For instance, NO_x (NO and NO_2) is produced in a mixture of N_2 and O_2 under the effect of plasma (Abdelaziz et al., 2023; Pei et al., 2019; Van Alphen et al., 2022). Furthermore, plasma serves as a highly responsive state of matter without the requirement of any activation or deactivation period. Plasma-based NF can be coupled with a renewable energy system for enhancement in the operating efficiency, especially when overcharging an energy storage system (Bogaerts and Neyts, 2018; Trinh et al., 2022). Although the plasma technology provides a blend of reactive species capable of performing NF at low temperatures and atmospheric conditions, the current state of art in plasma-based NF shows high energy consumption by plasma compared to that of well-established Haber-Bosch process. (Patil et al., 2015; Tsonev et al., 2023; Wang et al., 2017). Consequently, the recent surge in the investigation of atmospheric plasma for NF process as well as gas conversion is observed for improvement in plasma technology (Abdelaziz and Kim, 2020; Bahnamiri et al., 2021; Ramakers et al., 2019).

Numerous atmospheric plasma sources have successfully converted atmospheric N_2 into other nitro compounds. Plasma-induced NF was initially achieved by the Birkeland-Eyde process at an industrial scale in 1903; the process produced nitric acid by introducing air into an electric arc zone and then absorbing it in water (Rouwenhorst et al., 2021). The large energy requirement was a major reason for the ineffectiveness of this process. Since then, several types of thermal or nonthermal plasma have been extensively investigated for NO_x production (Patil et al., 2015; Zhou et al., 2021). Thermal plasmas can achieve good conversion and high product concentration, but considerable energy is consumed in heating bulk gas molecules. In comparison, nonthermal plasma requires lesser amount of input energy for heating gas molecules along with achieving sustainable gas conversion. Consequently, nonthermal plasma is an enticing substitute for thermal plasma due to its promising energy efficiency and favorable operating conditions. For instance, Abdelaziz et al. (Abdelaziz and Kim, 2020) demonstrated that a pulsed dielectric bed discharge (DBD) reactor was effective in the generation of NO_x or N_2O_5 in the range of 300–600 K; these concentrations were largely affected by the operating temperature and humidity. Ma et al. (2021) achieved NO_x production at a low energy cost of 15.9 MJ/mol with a 67.9% NO selectivity in a DBD reactor packed with $BaTiO_3$ catalyst. Aqueous ammonia was achieved with plasma jet treatment of N_2 gas containing water vapor; after the treated gas was dissolved in water (Gorbanev et al., 2020). Although, DBD plasma has been broadly used in NO_x synthesis due to their high power along with ease of coordination with catalysts; it has limited gas treatment volume and lower yield (Chen et al., 2021b). Overall, there has been an increase in investigations targeting the industrial application of nonthermal plasma for NF.

Recently, gliding arc (GA) plasma stands out to be a potential reactor choice for numerous gas conversions including NF operation (Jardali et al., 2021; Kim and Chun, 2014; Van Alphen et al., 2021). Operating between the non-equilibrium and equilibrium conditions, GA plasma can induce the numerous chemical reactions at low temperature due to the sufficient vibrational excitation of the molecules (Denra et al., 2023), that are otherwise thermodynamically unfavorable. Several works illustrate the successful operation of arc plasma in NF with favorable energy consumption. Particularly, Patil et al. (2016) performed the synthesis of NO_x in a mini-scale GA reactor reaching around 1% concentration of NO_x at energy consumption of 10 kWh/kg of NO_x , wherein the NO to NO_2 ratio in the product was found to be largely affected by the feed ratio. Chen et al. (2021a) used a rotational GA plasma for the synthesis of NO_x ; wherein flow rate was observed to be the major parameter affecting the NO_x concentration and O_2 concentration being the most important in optimizing energy consumption. Van Alphen et al. (Van Alphen et al., 2022) used a novel effusion nozzle approach to perform NO_x production in a rotating GA, wherein up to 5.9% NO_x concentrations were achieved at an energy consumption of

2.1 MJ/mol. Tsonev et al. (Tsonev et al., 2023) studied NO_x production at high pressures (2–4 atm) in arc plasma achieving 68.9 g/h production rate at an energy consumption of 1.8 MJ/(mol N). Li et al. (2023) implemented a two-dimensional GA plasma using AC pulsed mode operation for the successful generation of NO_x which showed a 15% improvement in energy efficiency compared to the continuous operation of plasma.

The objective of this study is to investigate the parameters affecting NO_x formation in a rotational GA reactor powered by an AC source with a low frequency of 60 Hz. Since nearly all the works performed in plasma-based NF used high frequency AC source or a DC power supply; this work is intended to study the technology at low frequency for easier practical applications. The reactor used was small in structure and designed in lab which makes it a great choice for easy and rapid N_2 fixation tool. Moreover, the effect of temperature of reactor on NO_x formation was studied to obtain a stable yield for prolonged operation. Overall, the research focuses on NF in the form of nitrogen oxides using a mixture of N_2 and O_2 aided by atmospheric arc plasma. The NO_x concentration obtained in the experimental results were compared with the equilibrium NO_x formation (from thermal oxidation of N_2) at thermal conditions which showed the effectiveness of plasma process at low temperatures. Experiments were conducted to investigate the effect of various input parameters (input power, gas flow rate, inlet gas composition (by volume fraction), water content in feed gas) on NO_x yield. The work also shows the effective conversion of the NO_x to nitric acid (HNO_3) with the aid of plasma. Thus, this system coupled with renewable energy sources for plasma generation can be successfully implemented for NF at remote locations.

2. Experimental section

2.1. Rotational gliding arc reactor geometry

The schematic illustration of the rotational GA reactor used in this study is depicted in Fig. 1(a) showing the internal dimensions and configuration. The reactor consists of an aluminum cone shaped electrode (active length = 45 mm, angle = 5°) connected to the high voltage. It was enclosed in a stainless-steel tube with 11 mm internal diameter serving as a ground electrode. The cone shaped structure was enclosed in a rectangular Teflon structure (4.8 cm \times 3.95 cm \times 3.95 cm). The part of Teflon surrounding the cone is hollow to fit the grounded cylindrical tube. The entire GA structure is shown in Supplementary information (SI) Fig. S1. The main inlet tube is branched into two tangential inlets to the reactor placed diagonally opposite to each other. The advantage of this reactor lies in the conical structure of the electrode, facilitating a rotational GA that extends the gas retention time within the plasma discharge zone. Prolonged operation in typical plane-to-plane GA reactor leads to increased temperature, potentially causing the electrode to expand in size and consequently halting the operation. However, the cone shaped electrode is less susceptible to temperature effects, ensuring stable long-term operation. Additionally, this reactor offers promising potential for easy upscaling compared to the plane-to-plane GA plasma electrode.

2.2. Experimental setup

The plasma for NO_x generation was driven by an AC 60-Hz high voltage, which was generated with a frequency converter (Sampoong Power Co., Ltd., Korea) along with a transformer (Model: DKNE-18, Korea). The feed gases (N_2 and O_2) were supplied to the GA reactor using Mass Flow Controllers (AFC500, Atovac Co., Korea). The splitting of the N_2 flow with a fraction being passed through de-ionized (DI) water was used to control the moisture content in the feed gas; the moisture content was measured at the reactor outlet with inlet moisture content measured before turning on plasma. Moreover, no water condensation has been observed in this work. Fig. 1(b) shows the schematic of the

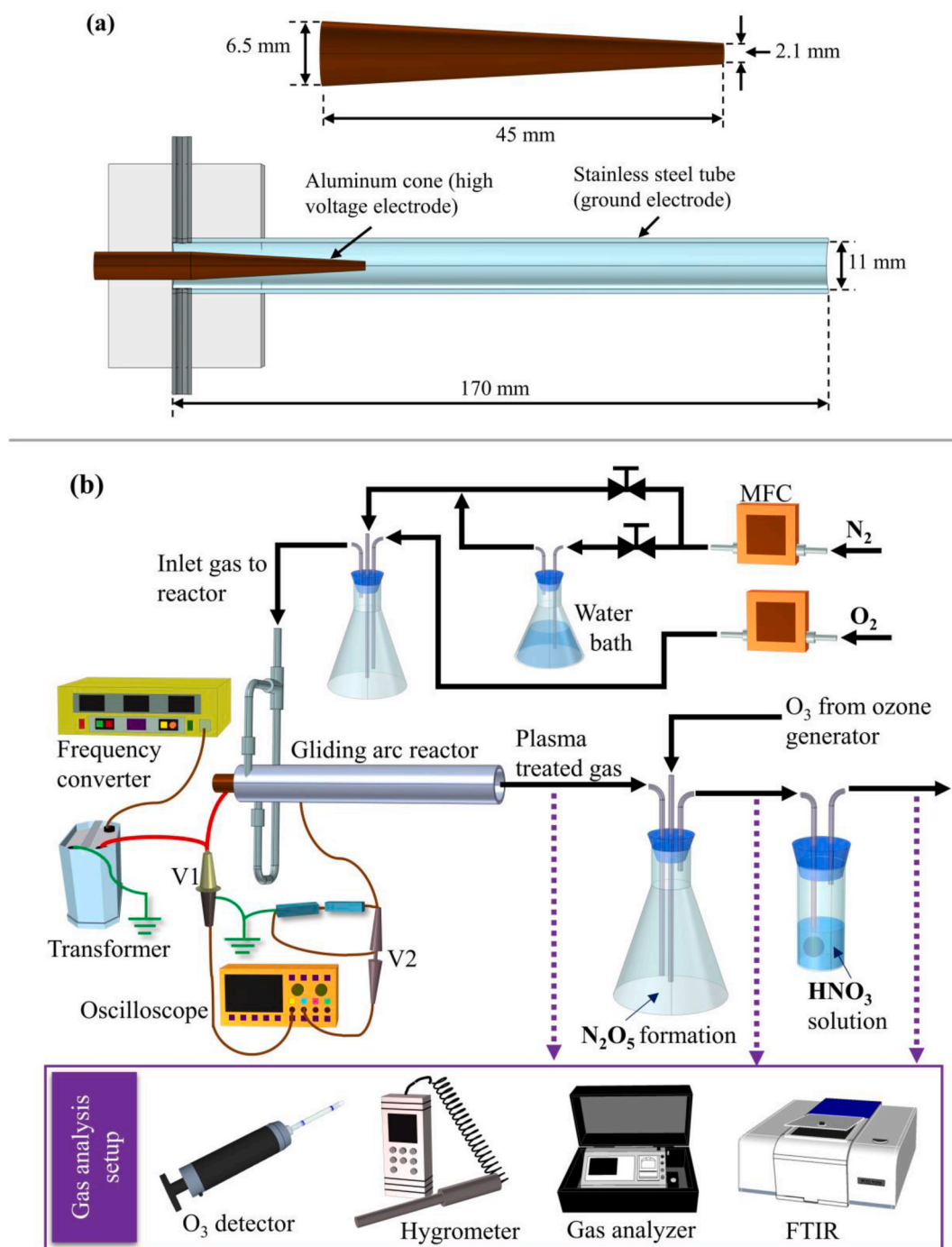


Fig. 1. Schematic diagram of (a) gliding arc reactor demonstrating the dimensional geometry of the high voltage and ground electrode (b) experimental setup.

experimental setup. The inlet gases enter tangentially into the reactor generating a vortex around the high voltage electrode. The plasma-treated gas from GA reactor containing NO and NO₂ was mixed with O₃ in a mixing flask to form N₂O₅. The O₃ required in this work was generated using a DBD reactor as shown in Fig. S2; details are included in SI section S.2. Finally, the gas mixture was bubbled through 100 ml of DI water resulting in the formation of HNO₃ solution.

A digital oscilloscope (Tektronix, DPO 3034, USA) was used to record the waveforms of the GA reactor using a high-voltage probe 1000:1 (Tektronix, P6015A, USA). A low-voltage probe (Tektronix, TPP0101, USA) was connected to the ground electrode along with two 1 kΩ resistors connected in series. The electrical waveform of the GA reactor is shown in Fig. S3. A gas analyzer (EN2, ecom GmbH, Germany) and a

Fourier transform infrared spectrophotometer (FTIR-7600, Lambda Scientific, Australia) was used to study the compositions of different samples present in the gas. Moreover, N₂O was not found in the plasma-treated gas. The O₃ concentrations were monitored using Ozone detector tubes (GASTEC Corp., Japan). The water content in the gas was monitored using a hygrometer (Traceable, 4185, USA). The surface temperature of the GA reactor was studied using thermal imaging infrared camera (FLIR-E6390, FLIR Systems Inc., Sweden). A ceramic temperature probe equipped with a digital temperature controller (Hanyoung ED6, Hanyoungnux Co., Ltd, Korea) was used for recording the gas temperature. A digital pH meter (Starter300, Ohaus corp., USA) along with pH paper (Macherey-Nagel GmbH & Co. KG, Germany) were utilized in confirming the pH of the HNO₃ solution.

2.3. Data analysis

The NO_x ($\text{NO} + \text{NO}_2$) concentrations were measured periodically for a fixed range of time. The analyzation of the results required the implication of several terms which can be defined as follows:

$$\text{Average NO or NO}_2 (\text{ppm}); \bar{x} = \frac{\sum_{i=1}^n x_i}{n} \quad (1)$$

$$\text{Error bar} = \sqrt{\frac{\sum_{i=1}^n (x_i - \bar{x})^2}{n - 1}} \quad (2)$$

$$\text{Average NO}_x (\text{ppm}) = \text{Average NO} (\text{ppm}) + \text{Average NO}_2 (\text{ppm}) \quad (3)$$

$$\text{NO}_x \text{ production (L/min)} = \text{Average NO}_x (\text{ppm}) \times \left(\frac{\text{Flow rate (L/min)}}{10^6} \right) \quad (4)$$

$$\text{NO}_x \text{ production (mol/s)} = \frac{\text{NO}_x \text{ production (L/min)}}{24.45 \times 60} \quad (5)$$

Here 24.45 represents the volume of a mole of gas or vapor at 1 atm and 25 °C.

$$\text{NO}_x \text{ yield (mol/MJ)} = \frac{\text{NO}_x \text{ production (mol/s)}}{\text{Applied Power (W)}} \times 10^6 \quad (6)$$

$$\text{Selectivity of NO (or NO}_2) = \frac{\text{Average NO (or NO}_2)}{\text{Average NO}_x} \quad (7)$$

$$\text{Energy consumption (MJ/mol)} = \frac{1}{\text{NO}_x \text{ yield (mol/MJ)}} \quad (8)$$

$$\text{Specific energy input, SEI} \left(\frac{\text{J}}{\text{L}} \right) = \frac{\text{Applied power (W)}}{\text{Total flow rate (L/min)}} \times 60 \quad (9)$$

2.4. Thermal NO_x formation

To evaluate the energy efficiency of the rotational GA plasma for NF, a comparison of energy consumption between thermal reactions and plasma reactions for NO_x generation was performed. Herein, N_2 and O_2 were used as the precursors of NO_x production in the plasma discharge. Therefore, the theoretical method chosen in this case was the thermal oxidation of N_2 , keeping in mind that the pioneer materials remain the same in both cases. The comparison was conducted through amounts of NO_x formation as a function of energy consumption (SEI). Herein, the amounts of NO_x by thermal reactions were estimated through partial pressures equilibrium constants (K_p , atmospheric pressure) at the corresponding temperature (T_c); equilibrium constants of reaction between N_2 and O_2 for the formation of NO and NO_2 at various temperatures were taken from (Cooper and Alley, 2010). The detailed process is shown in SI section S.8. The T_c was estimated as an equilibrium temperature of the N_2 and O_2 mixture when using the same amount of energy consumed by plasma process for heating the mixture from room temperature (~25 °C)

to reach T_c , $\text{SEI} = \int_{298}^{T_c} C_p dT$. The SEI of air, N_2 , and O_2 was calculated by

Eq. (10) that was adapted from ref. (Saud et al., 2020); these constants (C_x) were taken from ref. (Prudich et al., 2008). In the case of a mixture of N_2 (x) and O_2 ($1-x$), the SEI was the sum of the individual SEI multiplied by its fraction (Lee et al., 2023), as shown in Eq. (11). The standard molar enthalpy of reactions ($\Delta_f H_r$ or formation) for NO and NO_2 at 298.15 K was 91.3 and 33.2 kJ/mol, respectively (Haynes, 2015), suggesting endothermic reactions. Consequently, in actual operation, the energy consumption at T_c for thermal reactions will be the sum of SEI

(T_c) + $n_{\text{NO}} \Delta_f H_{T_c}(\text{NO})$ + $n_{\text{NO}_2} \Delta_f H_{T_c}(\text{NO}_2)$ (n_{NO} and n_{NO_2} represents the amount of NO and NO_2 formation), which is larger than that of SEI (T_c). Since the concentration of NO and NO_2 formation is in thousands ppm level in the examined SEI range, amount of NO_x is negligible compared to bulk gases (N_2 and O_2). In other word, $n_{\text{NO}} \Delta_f H_{T_c}(\text{NO})$ + $n_{\text{NO}_2} \Delta_f H_{T_c}(\text{NO}_2)$ is negligible compared to SEI (T_c) in this work. Thus, for facilitating calculation, the equilibrium temperature for thermal reaction under the same SEI by plasma reactions was approximately equal to T_c , as defined above.

$$\text{SEI}_{eq} \left(\frac{\text{J}}{\text{kmol}} \right) = \left(C_1 T + C_2 C_3 \coth \left(\frac{C_3}{T} \right) - C_4 C_5 \tanh \left(\frac{C_5}{T} \right) \right) \Big|_{298}^{T_c} \quad (10)$$

$$\text{SEI}_{eq}(x\text{N}_2; (1-x)\text{O}_2) = x \text{SEI}_{eq}(\text{N}_2) + (1-x) \text{SEI}_{eq}(\text{O}_2) \quad (11)$$

$$\frac{1}{2}\text{N}_2 + \frac{1}{2}\text{O}_2 \rightleftharpoons \text{NO} \quad \Delta_f H_r = 91.3 \text{ kJ/mol} \quad (\text{R1})$$

$$\frac{1}{2}\text{N}_2 + \text{O}_2 \rightleftharpoons \text{NO}_2 \quad \Delta_f H_r = 33.2 \text{ kJ/mol} \quad (\text{R2})$$

Here, owing to the gas volume in this work being determined or calculated at 25 °C and atmospheric pressure (room conditions), the conversion factor of SEI from J/kmol to J/L was 1:24,450.

3. Results and discussion

3.1. Effect of input power

The NO and NO_2 were monitored at the outlet of GA reactor under various applied powers. Fig. 2(a) displays the average NO_x generated by

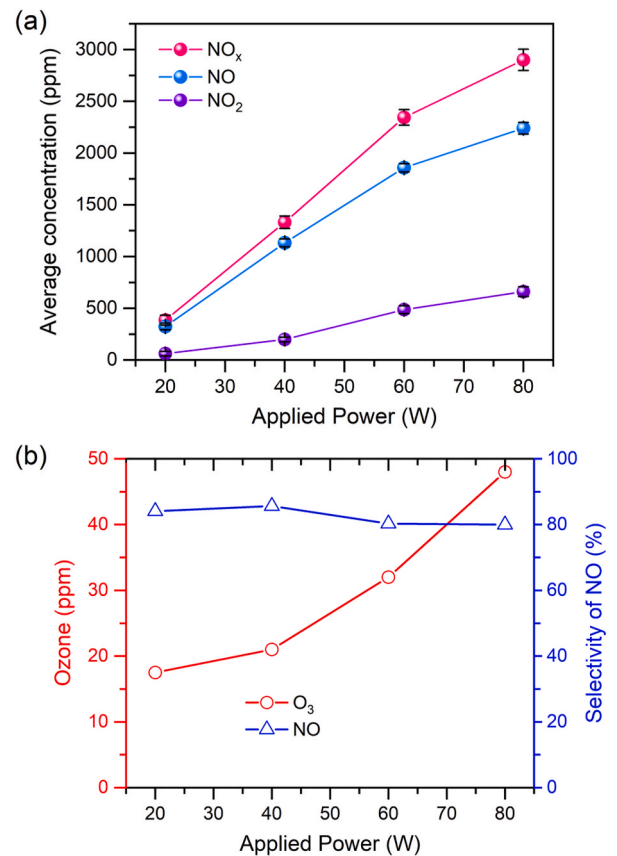


Fig. 2. Effect of applied voltage on (a) concentration of NO , NO_2 , and overall NO_x formation and (b) selectivity of NO and O_3 concentration (total flow rate = 2 L/min with $\text{N}_2:\text{O}_2 = 4:1$).

GA at steady state. The evolution of NO, NO₂ and NO_x over time at varied applied power (20–80 W) is shown in SI Fig. S4(a–d); it shows that the concentrations gradually decreased and reached steady state within 30 min of operation. Herein, the total gas flow rate was maintained at 2 L/min that consisted of 80% N₂ and 20% O₂ (N₂/O₂ = 4:1). With an increase in applied power, the average NO, NO₂ and overall NO_x concentration increased almost linearly, as shown in Fig. 2(a). For an input power of 20 W, the GA reactor generated an average NO_x of around 385 ppm that increased to almost 2883 ppm at 80 W; the NO_x generation was enhanced 7.5 times when the applied power was raised by 4 folds. Increase in applied power generates more atomic N, O, and reactive species (like NO[•], NO⁺, O₃, O⁺, N₂⁺, and N₂⁺) possessing high oxidizing properties resulting in enhancement of NO_x production. It is also evident from the increment of O₃ with respect to applied power, as shown in Fig. 2(b). The increasing O₃ concentration at higher applied power is in line with a gradual decrease in NO selectivity from 85.6% to 80.0%; a plausible reason is that more oxidation of NO to NO₂ by reaction with O[•] or O₃ (reactions R4, 7–8).



Moreover, higher energy input results in higher concentration of excited species that in turn leads to frequent collision of the oxygen species leading to O₃ formation. Despite the possibility of temperature rise due to increased energy input, the O₃ concentration showed an upward trend in response to increased input power. This can be attributed to the rapid cool down of gas and short residence time in the actual discharge zone, where the gas temperature could be highest, which limits the backward reaction of O₃ formation.

3.2. Effect of flow rate

The effect of flow rate on NO_x production was observed at various flow rates and applied power, as shown in Fig. 3(a). The NO and NO₂ concentration dropped by around 46 and 67 % in average, respectively, when flow rate was increased from 2 to 4 L/min. It can be attributed to the reduced residence time as well as reduced O₃ concentration (Fig. 3(b)); the residence time decreased from 0.09 to 0.04 s and average O₃ concentration dropped by 38 % on increasing flow rate from 2 to 4 L/min. The evolution in NO_x generation over time with increase in applied power for 3 and 4 L/min is shown in Figs. S5 and S6, respectively in SI (Section S.5). The selectivity of NO increased from 80.0% for 2 L/min to 87.5% at an applied power of 80 W when the total flow rate was increased to 4 L/min, as shown in Fig. 3(b). Based on these phenomena, it can be hypothesized that the reactions for the formation of NO_x, such as R3–8, occurred mostly in and post-close discharge zone. Overall, the increase in flow rate resulted in large gas velocity and reduced the gas treatment duration in the plasma. The relatively small volume of the reactor limited the volume of gas treatment; thus, a higher flow rate of gas was not applicable. Similarly, at a gas flow rate less than 2 L/min, uniform and stable gliding plasma was not observed; hence, a minimum gas flow rate of 2 L/min was chosen for this work considering the reactor configuration, plasma source type and plasma frequency. The maximum concentration of NO_x obtained was around 2883 ppm at an applied power of 80W and flow rate of 2 L/min.

According to the above results, the concentration of NO_x reduced at a higher flow rate, and higher NO_x concentration was obtained at a larger

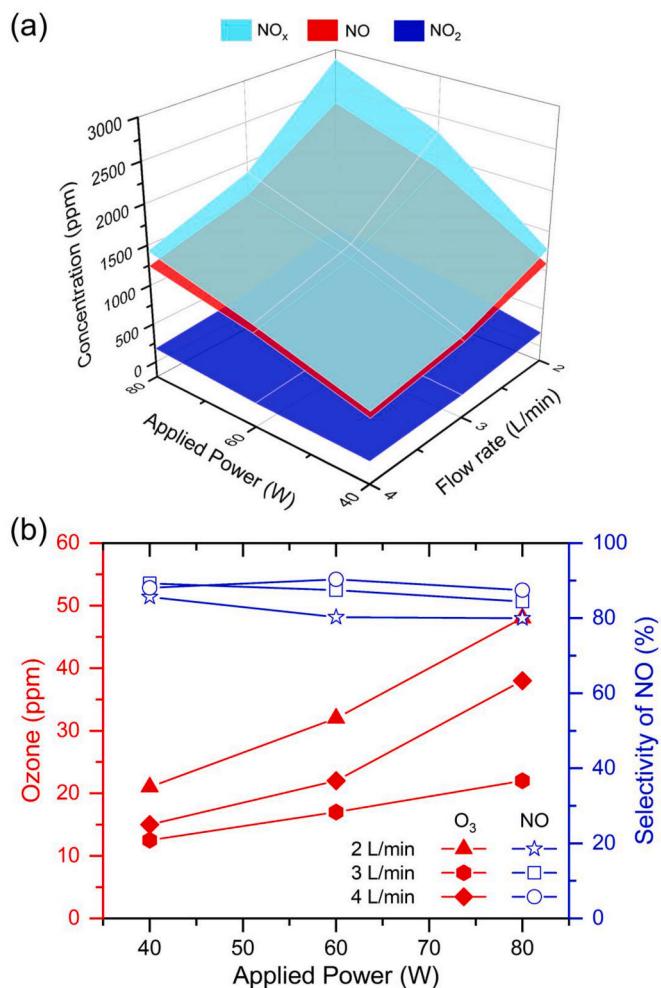


Fig. 3. Effect of total flow rate on (a) concentration of NO, NO₂, and overall NO_x formation and (b) selectivity of NO and O₃ concentration under various applied power (N₂:O₂ = 4:1).

energy input. Meanwhile, the amount of NO_x production yield is a multiplication of the total flow rate with NO_x concentration. Therefore, to evaluate the effect of total flow rate and applied power on the nitrogen oxidation process, NO_x production yield and energy consumption were plotted under various flow rates conjugated with applied power

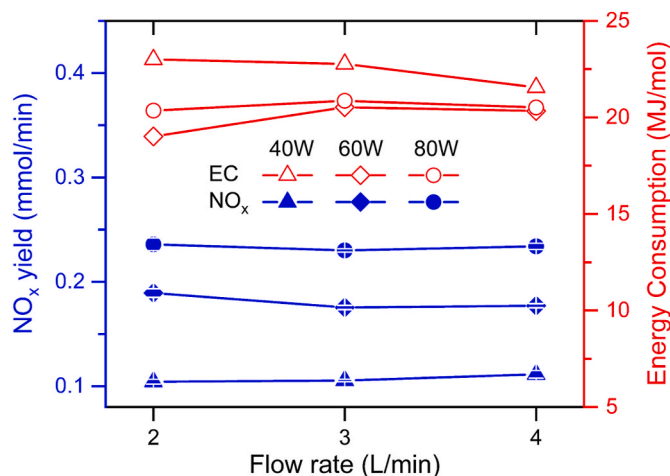


Fig. 4. NO_x yield and energy consumption as a function of total flow rates under various applied power (N₂:O₂ = 4:1).

(40–80 W), as shown in Fig. 4. This figure indicates that NO_x production yield slightly changed under the fluctuation of total flow rate from 2 to 4 L/min at the same applied power. However, the energy consumption for NO_x production is observed to be lowest at an applied power of 60 W under the flow rate fluctuation. To sum up, the energy consumption negligibly changed by varying the flow rate from 2 to 4 L/min; meanwhile, the energy consumption depended on applied power. The lowest energy consumption was obtained at 19 MJ/mol of NO_x at the total flow rate of 2 L/min and applied power of 60 W, considering the use of input power for the calculation of energy consumption.

3.3. Effect of O_2 content

The NO_x yield with respect to O_2 content in the feed gas was observed by varying O_2 from 20 to 50 % i.e., N_2/O_2 ratio varied from 4 to 1, respectively. It can be clearly observed from Fig. 5(a) that maximum NO_x of 3086 ppm was generated at O_2 content of 40 % at an applied power of 80 W. Even though the O_3 production at 50 % O_2 content was higher than in the case of 40 % O_2 content, as evident by Fig. 5(b), the NO_x production rate was highest at 40 % O_2 content with a value of 4.2 $\mu\text{mol/s}$ at an applied voltage of 80 W [Fig. 5(c)]. The trend in NO_x generation with varying N_2 to O_2 ratio at different input power over time is shown in SI section S.6; Figs. S7 and S8. Theoretically, the presence of equimolar proportion of N_2 and O_2 in the feed gas should result in higher

yield of NO_x compared to other cases. However, experimental results show that NO_x generation was higher when the amount of N_2 was slightly higher than O_2 fraction. Although the NO concentration decreased with increase in the O_2 fraction resulting in the highest NO yield for 4:1 N_2 to O_2 ratio, the NO_2 formation was relatively higher for 1:1 and 3:2 N_2 to O_2 ratio. A similar trend in NO_x formation with respect to the N_2 to O_2 fraction was observed by Vervloessem et al. wherein the highest yield was observed in the presence of 60% N_2 in the feed (Vervloessem et al., 2020). Wang et al. (2017) examined the dependence of NO_x formation by GA plasma on N_2/O_2 ratio in feed by both experimental and modeling approach. They indicated that the optimized N_2/O_2 ratio for NO_x production is 1:1 for calculated data and 3:2–2:1 for experimental data. This is in strong agreement with the result, at 40% O_2 content corresponding to N_2/O_2 ratio of 3:2. However, when considering the energy consumption to generate NO_x , the lowest production cost came from the combination of 60 W applied power and 40 % O_2 content with an energy consumption of nearly 17.2 MJ/mol of NO_x , as seen in Fig. 5(d). Hence, further work was conducted under these conditions.

The dependence of NO and NO_2 fraction in the mixture of NO_x products is depicted in Fig. 6. This demonstrates that the selectivity of NO_2 increased linearly with the increase in O_2 content. Specifically, the selectivity of NO_2 was enhanced by approximately two times when O_2 changed from 20 to 50 % in the feed gas, e.g., the NO_2 selectivity

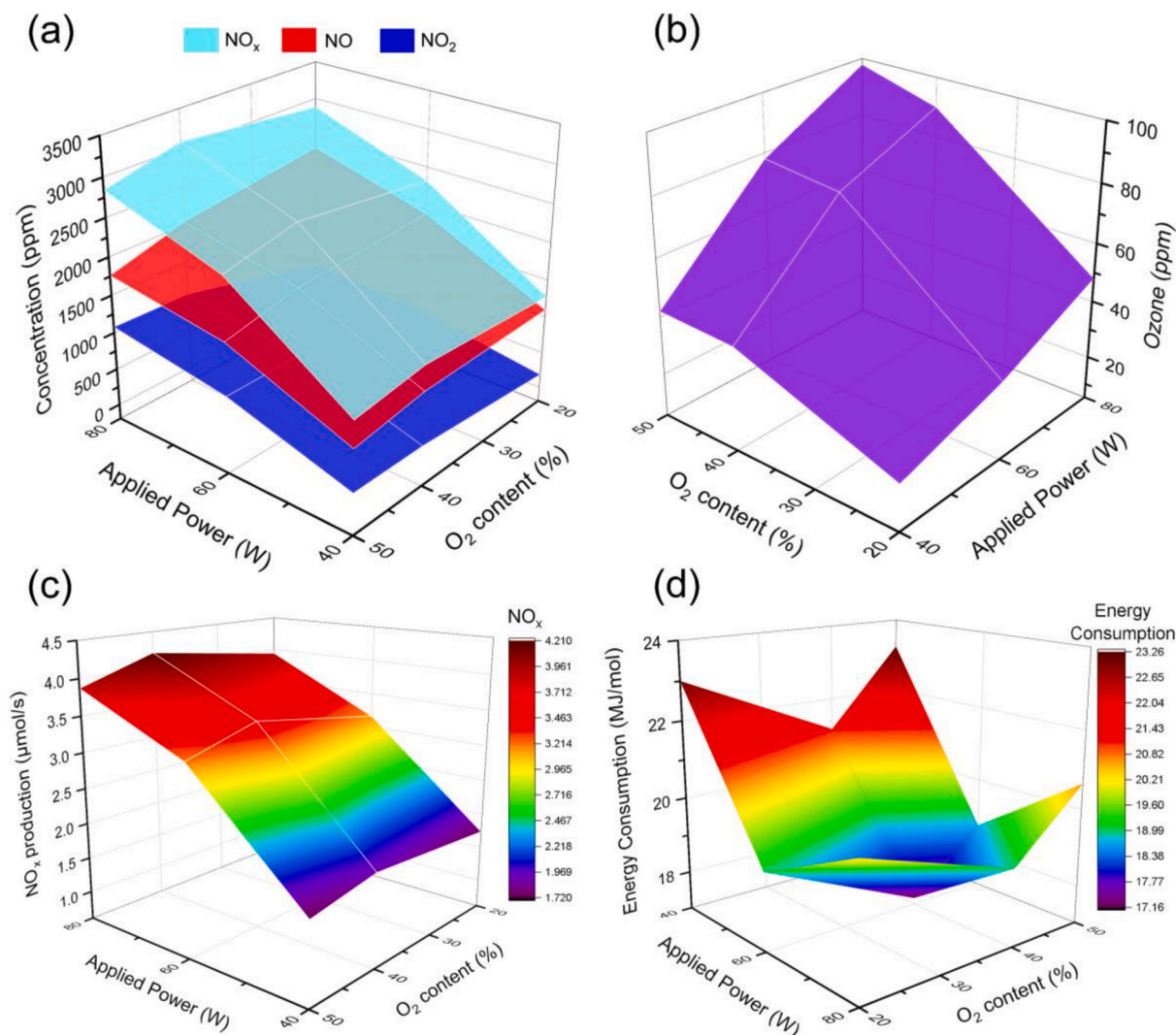


Fig. 5. Effects of oxygen content on nitrogen oxidation process by GA plasma (a) NO, NO₂ and NO_x concentration, (b) Ozone concentration, (c) NO_x production rate and (d) Energy consumption (total flow rate = 2 L/min).

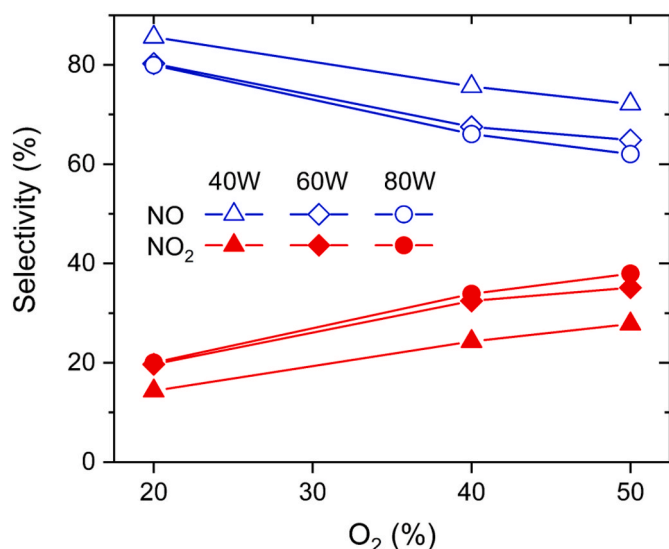


Fig. 6. Effects of oxygen content on selectivity of NO and NO_x (total flow rate = 2 L/min).

changed from 14.4% to 27.8% under an applied power of 40W. The trend in the enhancement of NO₂ fraction with the reduction in NO can be explained by the reactions of NO with O[•], O₃, and oxygen-excited species to form NO₂ (Wang et al., 2017), e.g., reactions R4-8. Furthermore, the NO₂ fraction also increased toward applied power, supporting the hypothesis that more input power produced more nitrogen and oxygen species. As a result, the concentration of NO₂ in the NO_x products can be adjusted by altering the O₂ content in the feed gas; the NO₂ fraction was around 38% for 50% O₂ content at an applied power of 80W.

3.4. Effect of water content

For practical applications of atmospheric pressure plasma, the plasma system maintains operating efficiency with water vapor, which is an essential factor. Furthermore, if the plasma system works well under a water content of up to 4%, the operating cost of the system will be reduced because ambient air can be considered a feed gas. The presence of water in plasma gases has both positive and negative effects on plasma processes. Specifically, Nguyen et al. (2020) presented that high performance of honeycomb plasma discharge can be obtained with the water vapor in the feed gas; unfortunately, it was also a reason for decreased plasma efficiency for the decomposition of contaminated compounds in gas treatment (Matyakubov et al., 2021; Nguyen et al., 2021; Saud et al., 2023). Regarding this aim, the dependence of NO_x and O₃ production was examined under different water contents (0–1.5 %) and applied powers (40–80W). The results are plotted in Fig. 7. The resultant NO_x formation with time is shown in Figs. S9 and S10.

Fig. 7(a and b) demonstrates that the concentration of NO, NO₂, overall NO_x, and O₃ decreased significantly with increased water content from 0 to 1.5%, i.e., 1388 ppm NO_x without water vapor to 911 ppm NO_x at 1.5% water; in other words, the NO_x reduced by 34.4% for applied power of 40 W. The decrease in NO_x and O₃ with the presence of water vapor in the plasma discharge can be explained by the consumption of nitrogen/oxygen excited species, radicals, energetic electrons, and excited species (M) in the GA plasma due to collisions and reactions with H₂O molecules. Therefore, substantial utilization of e⁻, N[•], O[•], and M interacted with H₂O rather than interacting among themselves to produce NO, NO₂, and O₃. This is also evident from the reduced peaks in the optical emission spectra of plasma in presence of water as shown in Fig. S11. Indeed, in this experiment, the water content was varied from 0.8 to 1.5% (equivalent to 8000–15,000 ppm); which

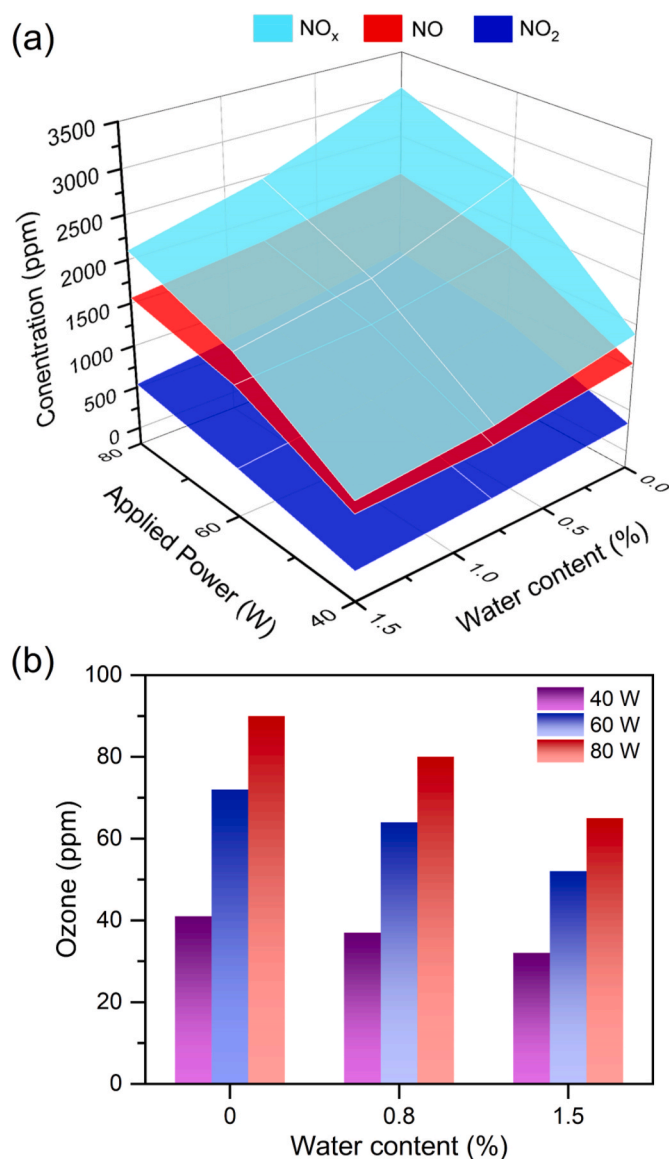


Fig. 7. Effect of water content on (a) NO_x and (b) ozone formation under various applied powers (total flow rate = 2 L/min; N₂:O₂ = 3:2).

was superior to the generated NO_x and O₃ concentration. Therefore, potential collision probabilities and formation of NO_x was reduced. Due to a significant decrease in NO_x product yield at higher water vapor, there is a decrease in energy efficiency under the presence of water vapor in the feed gas. According to the above NO_x formation hypothesis, the NO₂ formation is due to the oxidation of NO by reactive oxygen and ozone. The consumption of reactive oxygen by the interaction with H₂O molecules resulted in significant decrease in the NO₂ fraction in the NO_x product under the presence of water in feed. To validate, the selectivity of NO and NO₂ (fractions) was determined under varying water contents; the results are in line with the estimation, as shown in Fig. 8. For instance, the selectivity of NO and NO₂ was 75.65 and 24.35 %, respectively, in the absence of water; however, they were 84.27 and 15.72 % at a water amount of 1.5%. Overall, the presence of water vapor in the feed reduced the NO_x concentration, and NO₂ selectivity.

3.5. Comparison with thermodynamic NO_x production

Fig. 9 compares the equilibrium NO_x generation by thermal process (estimated data) and NO_x formation in GA plasma (experimental data)

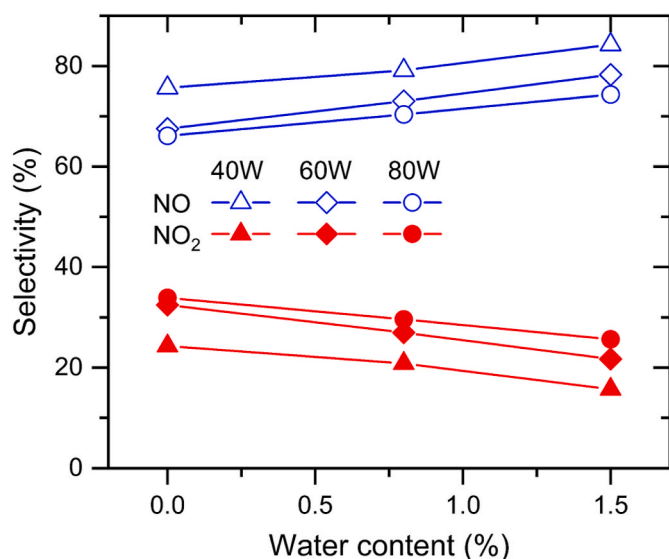


Fig. 8. Effect of water content on selectivity of NO and NO₂ under various applied powers (total flow rate = 2 L/min; N₂:O₂ = 3:2).

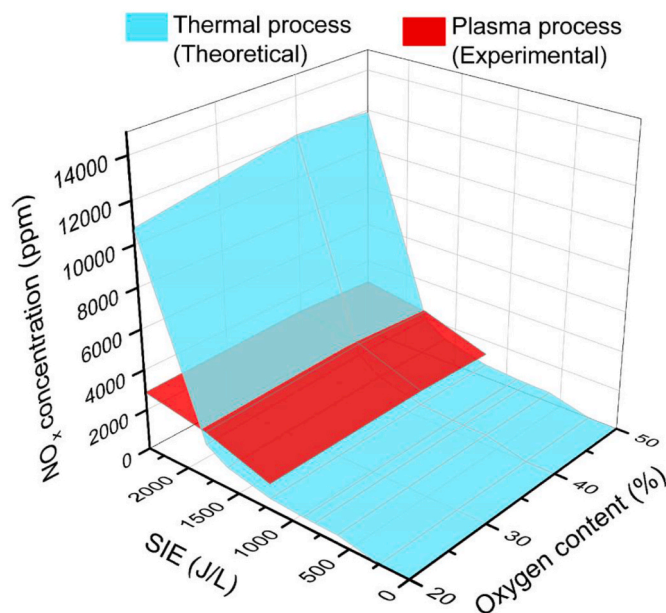


Fig. 9. A comparison between thermal process and gliding arc discharge for NO_x generation under various equivalent SEI and O₂ content (total flow rate = 2 L/min).

based on the same feed gas conditions and energy consumption. Herein, the energy is delivered directly to the plasma system for igniting and maintaining plasma reactions for NO_x formation. Meanwhile, the same energy amount is only used to heat the feed gas to obtain NO_x formation through thermal reactions; see Section 2.4 for the calculation method. Further details along with the results for the theoretical NO_x calculation are included in SI section S.8. The generation of NO_x at various N₂:O₂ feed ratios with increasing temperature along with their respective SEI are shown in Tables S3–S9 and Fig. S12. The comparison of NO_x evolution for plasma process at different SEI for various feed composition is included in Fig. S13. The NO_x production yield by GA was superior to the thermal process at the low SEI range (<1800 J/L) as seen in Fig. 9, suggesting superior NO_x generation by GA plasma. Unfortunately, when SEI reaches over 1800 J/L, the NO_x formation by thermal process increases sharply with SEI. Consequently, NO_x production yield by the

thermal process is superior to GA plasma for SEI ≥ 1800 J/L. The results demonstrate the noteworthy effectiveness of plasma technology in facilitating low-temperature nitrogen oxidation. However, under considerable energy input, the yield of plasma is lower than the thermal process, which is a disadvantage of plasma technology by the GA. This could be due to multiple reasons that include loss of considerable portion of input energy in self-heating (reactor and outlet gas heating), limited gas treatment in arc zone and low residence time. Therefore, the energy efficiency of plasma is lower than that of the thermal process at elevated energy input.

3.6. Effect of temperature

During plasma discharge, the reactor is self-heated by spending a part of the input energy [30]; consequently, the temperature of the reactor and outlet gas increases until the system obtains a steady state (Saud et al., 2021). In this study, the effect of temperature on NO_x formation by the GA reactor was performed using a self-heating method, i. e., covering the GA reactor with insulation. Consequently, the reactor with/without insulation was operated under the same conditions and the NO_x concentrations, gas temperature, and surface temperature were monitored for 120 min, as shown in Fig. 10.

The evolution of NO, NO₂, and overall NO_x is shown in Fig. 10(a); this figure revealed a decrease in NO, NO₂, and NO_x in presence of insulation with plasma-on time. Especially after 100 min, there is a decrease in NO_x with the insulation by approximately 10%, i.e., from 2340 ppm initial time to 1970 ppm NO_x at steady state. However, without insulation, there is a slight change in NO_x concentration with the plasma-on time up to 120 min, from 2400 ppm to 2340 ppm. As a result, the average NO_x concentration without insulation is higher than that of insulation, as shown in Fig. 10(b). The NO_x difference between the two conditions come from the insulation conditions that reduce the energy transferred from the GA reactor to the surrounding ambient air. Theoretically, the resultant increase in gas temperature should be accompanied by an increase in the NO_x concentration due to high temperature favoring thermal reactions. Whereas herein, we observed a rather decrease in the NO_x formation when the reactor was insulated. This effect is only explainable if the increase in the gas temperature had a negative effect on the plasma generated species resulting in the decrease in the overall yield. Since the pressure in the experimental conditions was supposed to be constant, the increase in temperature reduced the charged species in the plasma zone, and thus affecting the plasma density (Patil et al., 2018). Besides, the increase in temperature of the reactor surface increases its resistance thus reducing the current supplied and in turn decreasing the plasma density. Indeed, the gas and surface temperatures presented in Fig. 10(c and d) indicates that the surface temperature of both conditions is nearly similar. The thermal images of the surface temperature of GA reactor are included in SI Fig. S14. However, the gas temperature with insulation is higher than that of insulation absence, i.e., 245 °C and 187 °C for with and without insulation, respectively. The probe tip of the ceramic thermocouple was placed at a distance of 60 mm from the high voltage electrode for recording the gas temperature. Since plasma affects the gas temperature and surface temperature, the appearance of the discharge which was blue in color during initial period of ignition changes into red with lesser blue resemblance after an hour of plasma-on time, as shown in SI Fig. S15. Therefore, based on the above phenomena, it can be hypothesized that the decrease in NO_x formation in the case of insulation is a result of high gas temperature which affects the plasma density in the discharge zone.

To validate the long-term operation hypothesis of our reactor configuration, we continuously operated the reactor for 14 h. Fig. 10(e) illustrates the fluctuation of NO and NO₂ over time; the overall NO_x formation remains nearly consistent throughout the continuous 14-h operation. This supports the aforementioned hypothesis that the expansion of the electrode, caused by increased temperature, which

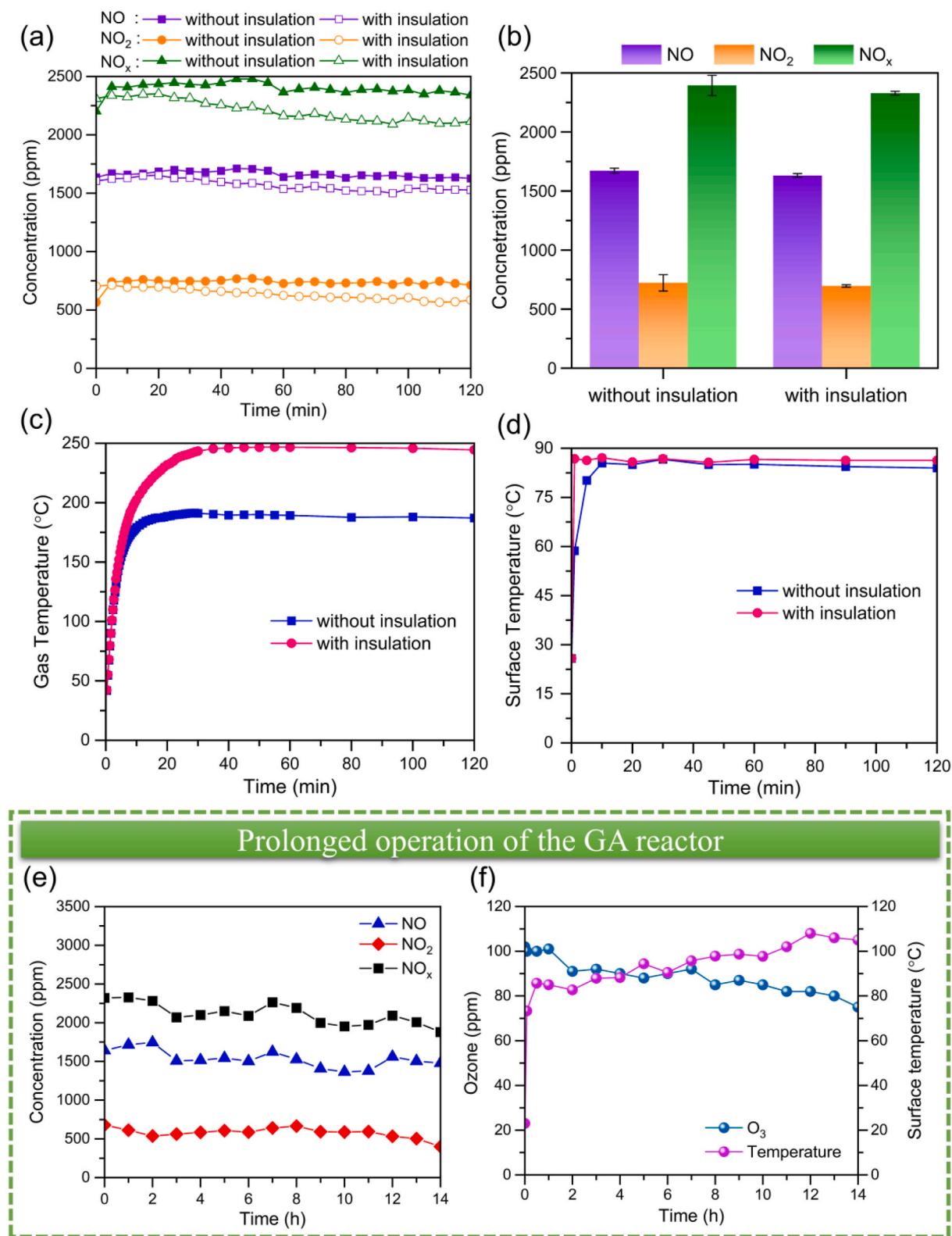


Fig. 10. (a–d) Effects of insulation on: (a) evolution of NO, NO₂, and NO_x concentration, (b) the concentration at steady state, (c) gas temperature, and (d) surface temperature, (e–f) Effect of long time GA operation on: (e) evolution of NO, NO₂, and NO_x and (f) Ozone concentration at the outlet and reactor surface temperature without insulation (total flow rate = 2 L/min; N₂:O₂ = 3:2, applied power = 60 W).

results in halting the operation of reactor, is negligible in the conical-shaped electrode within the GA discharge plasma. Fig. 10(f) shows the variation of the ozone at the reactor outlet and the reactor surface temperature. The ozone formation at the same time decreases slightly

over the 14 h period, probably due to increased temperature due to longer operation.

3.7. Formation of HNO_3

The pressurized NH_3 produced from the Haber Bosch process can be directly implemented into the soil as a fertilizer; however, it instantly vaporizes. The solution is to treat it with HNO_3 to form ammonium nitrate (NH_4NO_3), an involatile compound that can be used as fertilizer. In this work, the NO_x (NO and NO_2) generated through plasma based N_2 fixation via Zeldovich mechanism was ozonized to produce dinitrogen pentoxide (N_2O_5), which is readily soluble in water to form HNO_3 (Van Alphen et al., 2022). Herein, almost 1540 ppm of NO and 700 ppm of NO_2 generated by GA reactor at 2 L/min gas flow rate was ozonized by mixing it with 12,000 ppm of O_3 at 0.5 L/min flow rate, resulting in 2.5 L/min flow rate containing 1792 ppm NO_x ($\text{NO} = 1232$ ppm, $\text{NO}_2 = 560$ ppm) and 2400 ppm of O_3 . Ideally, O_3 required to produce N_2O_5 from NO_x is calculated from the equation below:

$$[\text{O}_3] = [\text{NO}] + \frac{[\text{NO}_x]}{2} \quad (12)$$



Herein, excess O_3 was fed to ensure complete conversion of NO_x to N_2O_5 ; the details of O_3 generation are included in SI section S.10 (Fig. S16). After the ozonation, the NO_2 peak completely disappeared and only N_2O_5 peak intensities were observed as evident by FTIR spectra of the gas before and after ozonation shown in Fig. 11(a). Using the Beer Lambert law, the concentration of N_2O_5 was calculated and was found to be around 866 ppm, which is almost 97 % of expected N_2O_5 ($1792/2 = 896$ ppm). The gas containing N_2O_5 was then bubbled through deionized water for 30 min at a flow rate of 2.5 L/min to produce HNO_3 via reaction R9. As N_2O_5 is highly soluble in water, it can be hypothesized that all N_2O_5 dissolves in water to form HNO_3 . To validate this, FTIR spectra comparison was done before and after reaction with water; the N_2O_5 peak disappearance was clearly visible in Fig. 11(a). Also, the change in the pH of the water from 6.5 to 1.36 indicated the formation of HNO_3 as shown in Fig. 11(b) (pH paper test included in SI section S.11 in Fig. S17). When back calculated using pH ($\text{pH} = -\log [\text{Concentration}]$), the HNO_3 concentration came around 0.044 M (712 ppm), which is equivalent to a concentration of 1424 ppm (equal to 80 % generated NO_x concentration). This acidic solution can then be reacted with NH_3 to

produce high N_2 containing fertilizer, i.e., NH_4NO_3 (N_2 content per mass = 35 %).

3.8. Overall mechanism for NO_x formation

The oxidation of N_2 to NO_x in the presence of O_2 under the effect of plasma is well known to follow the Zeldovich mechanism, which originally proposed that the formation of NO was processed via reactions between reactive atomic radicals with reactant gas molecules (Zeldovich Y, 1946). The overall mechanism is complicated due to the complex plasma mixture including several highly active charged species and radicals. The reaction pathway is initiated by the electron impact dissociation of the gas molecules into atoms. Fig. 12 demonstrates the basic NO_x formation pathway that can be deduced from this study. Although the electron energy in GA plasma is high but the plasma operated at room temperature offers the condition of activation of the small portion of the gas. Due to the lower energy bond in O_2 (5.15 eV) than in N_2 (9.79 eV), the density of atomic oxygen (O^\bullet) radical is much larger by 2–3 order of magnitude than the density of atomic nitrogen (N^\bullet) radical (Vervloessem et al., 2020). The Zeldovich mechanism is known to proceed by the following reactions:



The higher generation of O radicals implies that the occurrence of R10 is far superior to that of R11. The excitation of gas molecules in the plasma brought by the energy imparted to the particles by electrons generates a chemically reactive gas mixture. There are three excitation modes, including the rotational exciting mode with threshold energy smaller than 0.1 eV/molecule, the vibrational exciting mode with medium threshold energy from 0.1 to 1.5 eV/molecule and the electronical exciting mode with high threshold energy larger than 1.5 eV/molecule (Droege and Engelking, 1983; Maitre et al., 2020). At typical conditions of GA plasma which are characteristic by the range of electron energy from 0.6 to 4 eV and electron temperature of ~ 1 eV, 50–90% of this electron energy is transferred to induce the vibrational excitation of N_2 (Wang et al., 2017), triggering the activation of extremely strong triple $\text{N}\equiv\text{N}$ bond via the chain reaction R10. The high concentration of N_2

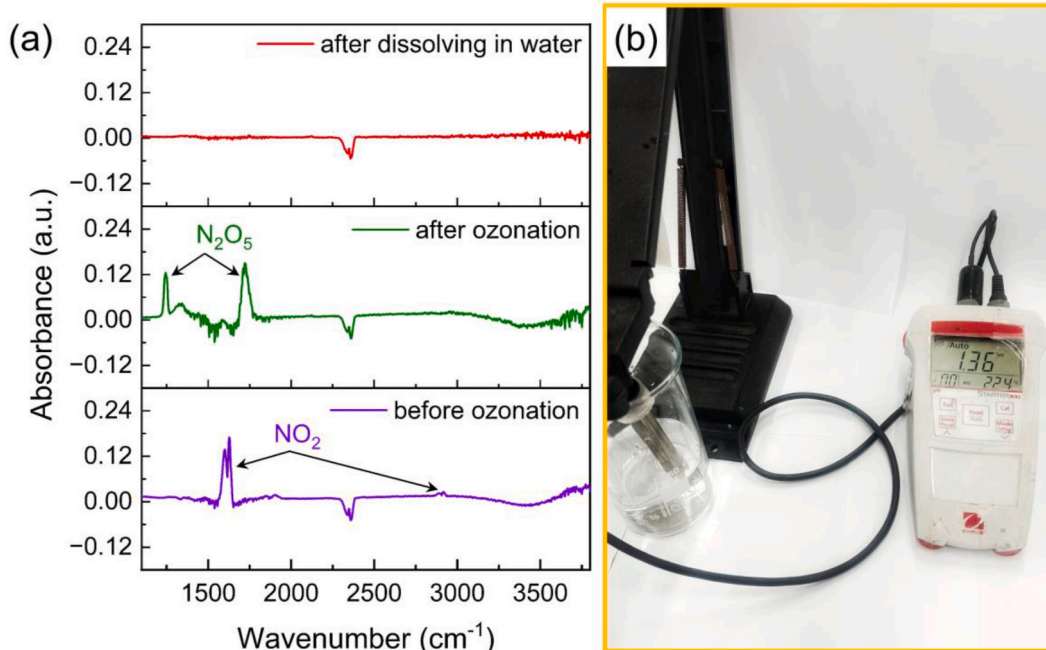


Fig. 11. (a) FTIR spectra confirming NO_2 , N_2O_5 presence and absence based on experimental conditions and, (b) Measured pH of the solution after N_2O_5 dissolution.

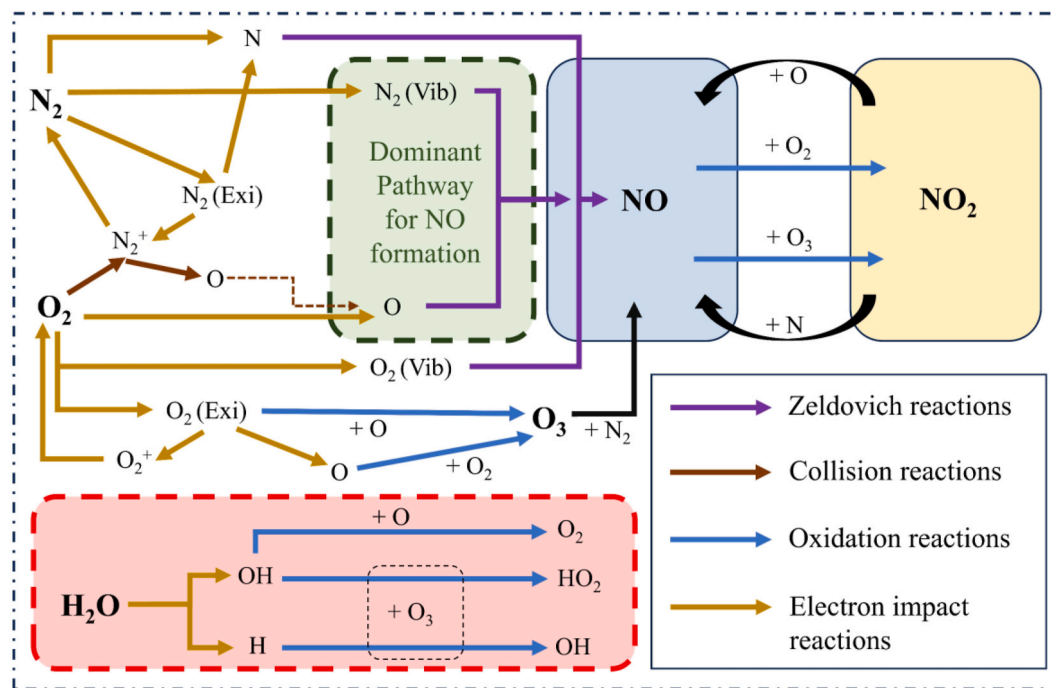


Fig. 12. A pathway depicting the predominant mechanism for NO_x formation in the gliding arc and the post arc zone.

(vib) excited species in the mixture can be a result of the vibrational temperature of N₂ being higher compared to its gas temperature (Liu et al., 2023). Being the dominant reaction, R10 is governed by the presence of O radicals in the mixture. Thus, the change in the O₂ content in the feed gas was found to directly influence the NO_x production. The NO_x generation was observed to rise with the increase in the O₂ content up to the N₂:O₂ of 3:2. A further change in the feed ratio to 1:1 decreased the NO generation since the presence of similar fraction N₂ and O₂ is known to promote the vibrational energy exchange between the species decreasing the concentration of vibrationally excited N₂ species. The electronically excited N₂ species in the plasma mixture can facilitate the formation of O atoms resulted by the collision with O₂ molecules. Thus, although the presence of higher concentration of N₂ in the case of 1:1 can boost the generation of O atoms, the NO formation decreases due to the reduction in the abundance of the N₂ (vib) excited species. Once NO is formed, it can be further oxidized with atomic oxygen radical or O₃ to produce NO₂ via the reaction (R7-8), contributing to the main pathway of NO₂ formation in GA plasma. However, reverse reactions from NO₂ with atomic radicals O[•] and N[•] (reaction R12-13) also contribute to the formation of NO, resulting in the equilibrium of NO and NO₂ in the total NO_x products.



Beside the pathway of NO_x generation, there also exists an important reaction that contribute negatively to the formation of NO_x, which is processed by the reaction (R14) between NO and N radical:



It was reported that a large portion of NO is eliminated upon interaction with atomic nitrogen radical in the plasma conditions, significantly reducing the yield of the process (Vervloessem et al., 2020). To utilize the important role of vibrational excitation of N₂ and O₂, the flow rate should be controlled to ensure the long enough residence time of those gas molecules in the electron-impact zone along with the optimized O₂ content to ensure a higher N₂ % in the feed stock.

The generation of O₃ from the reaction of atomic O with O₂

molecules further contributes to the enhancement in NO generation. Active N can readily convert into NO in presence of O₃ by the following reaction:



The surplus O₃ in the plasma treated mixture can also participate in the oxidation of NO into NO₂. O₃ is formed at high applied power (Fig. 2 (b)), which provides an extra source of oxygen radical upon colliding with any neutral species in the plasma zone. Although oxygen radicals can participate in the reverse reactions of NO and NO₂; an increment of oxygen radical density has more prominent effect to the oxidation of NO towards NO₂ which shifts the equilibrium of NO concentration and consequently enhancing the activation of N₂. It was reported that the NO₂ formation is 20 times higher if an air feed stock was diluted with 30% O₃ in the N₂ oxidation by GA plasma (Vervloessem et al., 2020). However, although the formation of O₃ is increased at higher O₂ fraction as is observed in Fig. 5(b), the N₂-to-O₂ vibrational exchange depletes the density of vibrationally excited N₂ and hinders the formation rate of NO_x. These factors therefore explain the optimized O₂ fraction of 40% in the feed to deliver the highest rate of NO_x formation (Fig. 5(a)).

The addition of water vapor in the feed was found to negatively impact the NO_x formation. Although, the presence of OH radicals can enhance the NO production by the extended Zeldovich mechanism as in reaction R16 (Van Alphen et al., 2022); but in this case the effect of reduction of charged species in the plasma by the presence of water seems to have had dominant effect on the NO_x production mechanism and in turn reduced the resultant yield.



The presence of water vapor can result in the decrease of energized electrons by absorbing considerable electronic energy in the plasma (Du et al., 2008); substantially reducing the amount of generation of N and O radicals and atoms in the discharge. Thus, the overall O₃ generation was also affected with the increase in water content in the feed gas. Moreover, the water molecules undergo electron impact dissociation to form H and hydroxyl (OH) ions. These ions can readily react with the ozone in the gas by the following reactions resulting in the further reduction of O₃

concentration (Du et al., 2008).



The presence of water molecules also increases the consumption of O atoms by the following reactions (Singleton et al., 2016); and in turn decreasing the probability of reaction R10.



Thus, the presence of moisture in the feed gas was found to be disadvantageous for NO_x formation in the GA reactor. Therefore, the overall critical surveillance of influence of the above parameters led us to the final optimized conditions for NO_x formation. A brief comparison of this work with respect to other NO_x formation works in plasma in terms of feed gas, power, yield, and energy consumption is included in SI section S.12.

4. Conclusions

This work focused on nitrogen oxidation to form NO and NO₂ (NO_x) through a rotational GA plasma at atmospheric pressure. Various parameters, applied power, total flow rates, O₂/water contents, and thermal insulation of the reactor, were investigated to understand their impact on NO_x generation. The experimental results demonstrated that energy input and total flow rate played vital role in regulating the NO_x production, while the composition of the feed gas significantly influenced the NO_x concentration. Specifically, NO_x yield decreased significantly with presence of water vapor but increased with higher O₂ content, enhancing NO₂ selectivity. The optimized gas composition of N₂:O₂ = 3:2, exhibited the highest NO_x generation based on the interaction between oxygen-reactive species and excited N₂ molecules. The comparison between the plasma and thermal process for NO_x generation (from N₂ and O₂) demonstrated the efficiency of plasma at low SEI level (<1800 J/L). However, as SEI increased (≥1800 J/L), the plasma process couldn't match the rising NO_x yield of the N₂ thermal oxidation process. In addition, the robustness of our reactor configuration was validated through a continuous 14-h operational test to confirm its long-term viability. The produced NO_x at the plasma stage coupled with an ozone generator resulted in conversion of NO_x into N₂O₅, subsequently forming a solution of HNO₃ when dissolved in deionized water. This underscores the potential application of rotational GA plasma in nitrogen fixation processes, showcasing promise for industrial nitrogen-related applications.

CRediT authorship contribution statement

Avik Denra: Writing – original draft, Writing – review & editing, Methodology, Investigation, Formal analysis, Data curation. **Shirjana Saud:** Writing – original draft, Writing – review & editing, Supervision, Investigation. **Duc Ba Nguyen:** Writing – original draft, Writing – review & editing, Investigation. **Quang Thang Trinh:** Writing – original draft, Writing – review & editing, Investigation. **Tuan-Khoa Nguyen:** Writing – review & editing. **Hongjie An:** Writing – review & editing. **Nam-Trung Nguyen:** Writing – review & editing. **Sosiawati Teke:** Writing – review & editing. **Young Sun Mok:** Writing – review & editing, Supervision, Funding acquisition.

Declaration of competing interest

The authors declare that they have no known competing financial interests or personal relationships that could have appeared to influence the work reported in this paper.

Data availability

The raw/processed data required to reproduce the above findings can be shared upon reasonable request to the corresponding author.

Acknowledgements

This work was supported by the Basic Science Research Program (2021R1A2C2011441) and **Regional Innovation Strategy (RIS) Program (2023RIS-009)** through the National Research Foundation funded by the Korean government (MSIT&MOE).

Appendix A. Supplementary data

Supplementary data to this article can be found online at <https://doi.org/10.1016/j.jclepro.2024.140618>.

References

- Abdelaziz, A.A., Kim, H.-H., 2020. Temperature-dependent behavior of nitrogen fixation in nanopulsed dielectric barrier discharge operated at different humidity levels and oxygen contents. *J. Phys. D Appl. Phys.* 53 (11), 114001.
- Abdelaziz, A.A., Teramoto, Y., Nozaki, T., Kim, H.-H., 2023. Performance of high-frequency spark discharge for efficient NO_x production with tunable selectivity. *Chem. Eng. J.* 470, 144182.
- Bahnamiri, O.S., Verheyen, C., Snyders, R., Bogaerts, A., Britun, N., 2021. Nitrogen fixation in pulsed microwave discharge studied by infrared absorption combined with modelling. *Plasma Sources Sci. Technol.* 30 (6), 065007.
- Bogaerts, A., Neyts, E.C., 2018. Plasma technology: an emerging technology for energy storage. *ACS Energy Lett.* 3 (4), 1013–1027.
- Chen, H., Wu, A.J., Mathieu, S., Gao, P.H., Li, X.D., Xu, B.Z., Yan, J.H., Tu, X., 2021a. Highly efficient nitrogen fixation enabled by an atmospheric pressure rotating gliding arc. *Plasma Process. Polym.* 18 (7), 2000200.
- Chen, H., Yuan, D., Wu, A., Lin, X., Li, X., 2021b. Review of low-temperature plasma nitrogen fixation technology. *Waste Dispos. Sustain. Energy* 3 (3), 201–217.
- Cherkasov, N., Ibadon, A.O., Fitzpatrick, P., 2015. A review of the existing and alternative methods for greener nitrogen fixation. *Chem. Eng. Process* 90, 24–33.
- Cooper, C.D., Alley, F.C., 2010. *Air Pollution Control: A Design Approach*. Waveland press.
- Denra, A., Matyakubov, N., Saud, S., Teke, S., Nguyen, D.B., Mok, Y.S., 2023. Essential features of gliding arc plasma for high-performance hydrocarbon selective catalytic reduction of NO_x at low temperatures. *Ind. Eng. Chem. Res.* 62 (25), 9595–9606.
- Droege, A.T., Engelking, P.C., 1983. Supersonic expansion cooling of electronically excited OH radicals. *Chem. Phys. Lett.* 96 (3), 316–318.
- Du, C.M., Sun, Y.W., Zhuang, X.F., 2008. The effects of gas composition on active species and byproducts formation in gas-water gliding arc discharge. *Plasma Chem. Plasma Process.* 28 (4), 523–533.
- Foster, S.L., Bakovic, S.I.P., Duda, R.D., Maheshwari, S., Milton, R.D., Minter, S.D., Janik, M.J., Renner, J.N., Greenlee, L.F., 2018. Catalysts for nitrogen reduction to ammonia. *Nat. Catal.* 1 (7), 490–500.
- Gorbanev, Y., Vervloessem, E., Nikiforov, A., Bogaerts, A., 2020. Nitrogen fixation with water vapor by nonequilibrium plasma: toward sustainable ammonia production. *ACS Sustainable Chem. Eng.* 8 (7), 2996–3004.
- Haynes, W., 2015. Thermochemistry, electrochemistry, and solution chemistry. *CRC Handbook of Chemistry and Physics* 130–131.
- Humphreys, J., Lan, R., Tao, S., 2021. Development and recent progress on ammonia synthesis catalysts for Haber–Bosch process. *Advanced Energy and Sustainability Research* 2 (1), 2000043.
- Jardali, F., Van Alphen, S., Creel, J., Eshtehardi, H.A., Axelsson, M., Ingels, R., Snyders, R., Bogaerts, A., 2021. NO_x production in a rotating gliding arc plasma: potential avenue for sustainable nitrogen fixation. *Green Chem.* 23 (4), 1748–1757.
- Kelly, S., Bogaerts, A., 2021. Nitrogen fixation in an electrode-free microwave plasma. *Joule* 5 (11), 3006–3030.
- Kelly, S., Verheyen, C., Cowley, A., Bogaerts, A., 2022. Producing oxygen and fertilizer with the Martian atmosphere by using microwave plasma. *Chem* 8 (10), 2797–2816.
- Kim, S.C., Chun, Y.N., 2014. Development of a gliding arc plasma reactor for CO(2) destruction. *Environ. Technol.* 35 (21–24), 2940–2946.
- Lee, S., Lee, J.W., Saud, S., Bhattarai, R.M., Mok, Y.S., Matyakubov, N., Nguyen, D.B., 2023. Comparison between in-/injected-plasma catalysis for enhancing hydrocarbon selective catalytic reduction of NO_x at low temperatures. *Chem. Eng. J.* 469, 143977.
- Li, S., van Raak, T., Kriek, R., De Felice, G., Gallucci, F., 2023. Gliding Arc reactor under AC pulsed mode operation: spatial performance profile for NO(x) synthesis. *ACS Sustain. Chem. Eng.* 11 (34), 12821–12832.
- Liu, J.L., Nie, L.L., Liu, D.W., Lu, X.P., 2023. Plasma for Nitrogen Fixation by Using N₂/O₂ Mixture: Reaction Pathway, Energy Flow, and Plasma Reactor. *Plasma Processes and Polymers*, e2300153.
- Liu, Q., Xu, T., Luo, Y., Kong, Q., Li, T., Lu, S., Alshehri, A.A., Alzahrani, K.A., Sun, X., 2021. Recent advances in strategies for highly selective electrocatalytic N₂ reduction toward ambient NH₃ synthesis. *Curr. Opin. Electrochem.* 29, 100766.

- Ma, Y., Wang, Y., Harding, J., Tu, X., 2021. Plasma-enhanced N₂ fixation in a dielectric barrier discharge reactor: effect of packing materials. *Plasma Sources Sci. Technol.* 30 (10), 105002.
- Maitre, P.-A., Bieniek, M.S., Kechagiopoulos, P.N., 2020. Plasma-enhanced catalysis for the upgrading of methane: a review of modelling and simulation methods. *React. Chem. Eng.* 5 (5), 814–837.
- Matyakubov, N., Nguyen, D.B., Saud, S., Heo, I., Kim, S.-J., Kim, Y.J., Lee, J.H., Mok, Y. S., 2021. Effective practical removal of acetaldehyde by a sandwich-type plasma-in-honeycomb reactor under surrounding ambient conditions. *J. Hazard Mater.* 415, 125608.
- Nguyen, D.B., Matyakubov, N., Saud, S., Heo, I.J., Kim, S.-J., Kim, Y.J., Lee, J.H., Mok, Y. S., 2021. High-throughput NO_x removal by two-stage plasma honeycomb monolith catalyst. *Environ. Sci. Technol.* 55 (9), 6386–6396.
- Nguyen, D.B., Shirjana, S., Hossain, M.M., Heo, I., Mok, Y.S., 2020. Effective generation of atmospheric pressure plasma in a sandwich-type honeycomb monolith reactor by humidity control. *Chem. Eng. J.* 401, 125970.
- Patil, B.S., Palau, J.R., Hessel, V., Lang, J., Wang, Q., 2016. Plasma nitrogen oxides synthesis in a milli-scale gliding arc reactor: investigating the electrical and process parameters. *Plasma Chem. Plasma Process.* 36 (1), 241–257.
- Patil, B.S., Peeters, F.J.J., van Rooij, G.J., Medrano, J.A., Gallucci, F., Lang, J., Wang, Q., Hessel, V., 2018. Plasma assisted nitrogen oxide production from air: using pulsed powered gliding arc reactor for a containerized plant. *AIChE J.* 64 (2), 526–537.
- Patil, B.S., Wang, Q., Hessel, V., Lang, J., 2015. Plasma N₂-fixation: 1900–2014. *Catal. Today* 256, 49–66.
- Pei, X., Gidon, D., Yang, Y.-J., Xiong, Z., Graves, D.B., 2019. Reducing energy cost of NO_x production in air plasmas. *Chem. Eng. J.* 362, 217–228.
- Prudich, M.E., Chen, H., Gu, T., Gupta, R.B., Johnston, K.P., Lutz, H., Ma, G., Su, Z., 2008. *Perry's Chemical Engineers' Handbook, Section 2 Physical and Chemical Data*. McGraw-Hill Publishing.
- Ramakers, M., Heijkers, S., Tytgat, T., Lenaerts, S., Bogaerts, A., 2019. Combining CO₂ conversion and N₂ fixation in a gliding arc plasmatron. *J. CO₂ Util.* 33, 121–130.
- Rouwenhorst, K.H.R., Jardali, F., Bogaerts, A., Lefferts, L., 2021. From the Birkeland–Eyde process towards energy-efficient plasma-based NO_x synthesis: a techno-economic analysis. *Energy Environ. Sci.* 14 (5), 2520–2534.
- Roy, N.C., Maira, N., Pattyn, C., Remy, A., Delplancke, M.P., Reniers, F., 2023. Mechanisms of reducing energy costs for nitrogen fixation using air-based atmospheric DBD plasmas over water in contact with the electrode. *Chem. Eng. J.* 461, 141844.
- Saud, S., Bhattarai, R.M., Nguyen, D.B., Neupane, S., Matyakubov, N., Lee, B., Kim, Y.J., Lee, J.H., Heo, I., Mok, Y.S., 2023. A comprehensive study on scaling up ethylene abatement via intermittent plasma-catalytic discharge process in a novel reactor configuration comprising multiple honeycomb monoliths. *Chem. Eng. J.* 454, 140486.
- Saud, S., Nguyen, D.B., Bhattarai, R.M., Matyakubov, N., Heo, I., Kim, S.-J., Kim, Y.J., Lee, J.H., Mok, Y.S., 2021. Dependence of humidified air plasma discharge performance in commercial honeycomb monoliths on the configuration and key parameters of the reactor. *J. Hazard Mater.* 404 (Pt B), 124024.
- Saud, S., Nguyen, D.B., Kim, S.-G., Lee, H.W., Kim, S.B., Mok, Y.S., 2020. Improvement of ethylene removal performance by adsorption/oxidation in a pin-type corona discharge coupled with Pd/ZSM-5 catalyst. *Catalyst* 10 (1), 133.
- Singleton, D., Carter, C., Pendleton, S.J., Brophy, C., Sinibaldi, J., Luginsland, J.W., Brown, M., Stockman, E., Gundersen, M.A., 2016. The effect of humidity on hydroxyl and ozone production by nanosecond discharges. *Combust. Flame* 167, 164–171.
- Steinberger-Wilckens, R., Sampson, B., 2019. Chapter 8 - market, commercialization, and deployment—toward appreciating total owner cost of hydrogen energy technologies. In: de Miranda, P.E.V. (Ed.), *Science and Engineering of Hydrogen-Based Energy Technologies*. Academic Press, pp. 383–403.
- Trinh, Q.H., Dinh, D.K., Lee, D.H., Nguyen, D.B., Mok, Y.S., Lee, W.G., 2022. Combination of atmospheric pressure plasma with catalysts for dry reforming of methane to value-added chemicals. In: Nanda, S., Vo, D.-V.N. (Eds.), *Innovations in Thermochemical Technologies for Biofuel Processing*. Elsevier, pp. 273–312.
- Tsonev, I., O'Modhrain, C., Bogaerts, A., Gorbaney, Y., 2023a. Nitrogen fixation by an arc plasma at elevated pressure to increase the energy efficiency and production rate of NO_x. *ACS Sustainable Chem. Eng.* 11 (5), 1888–1897.
- Van Alphen, S., Ahmadi Eshtehardi, H., O'Modhrain, C., Bogaerts, J., Van Poyer, H., Creel, J., Delplancke, M.-P., Snyders, R., Bogaerts, A., 2022a. Effusion nozzle for energy-efficient NO_x production in a rotating gliding arc plasma reactor. *Chem. Eng. J.* 443, 136529.
- Van Alphen, S., Jardali, F., Creel, J., Trenchev, G., Snyders, R., Bogaerts, A., 2021. Sustainable gas conversion by gliding arc plasmas: a new modelling approach for reactor design improvement. *Sustain. Energy Fuels* 5 (6), 1786–1800.
- Vervloessem, E., Aghaei, M., Jardali, F., Hafezkhani, N., Bogaerts, A., 2020. Plasma-based N₂ fixation into NO_x: insights from modeling toward optimum yields and energy costs in a gliding arc plasmatron. *ACS Sustainable Chem. Eng.* 8 (26), 9711–9720.
- Wang, Q., Gao, L., Li, Y., Shakoob, N., Sun, Y., Jiang, Y., Zhu, G., Wang, F., Shen, Y., Rui, Y., Zhang, P., 2023. Nano-agriculture and nitrogen cycling: opportunities and challenges for sustainable farming. *J. Clean. Prod.* 421, 138489.
- Wang, W., Patil, B., Heijkers, S., Hessel, V., Bogaerts, A., 2017. Nitrogen fixation by gliding arc plasma: better insight by chemical kinetics modelling. *ChemSusChem* 10 (10), 2145–2157.
- Wang, X.Y., Wang, B.D., Yin, S.Y., Xu, M.W., Yang, L.X., Sun, H., 2022. Highly efficient photocatalytic nitrogen fixation on bio-inspired triphase interface with improved diffusion of nitrogen. *J. Clean. Prod.* 360, 132162.
- Winter, L.R., Chen, J.G., 2021. N₂ fixation by plasma-activated processes. *Joule* 5 (2), 300–315.
- Wu, A.J., Yang, J., Xu, B., Wu, X.Y., Wang, Y.H., Lv, X.J., Ma, Y.C., Xu, A.N., Zheng, J.G., Tan, Q.H., Peng, Y.Q., Qi, Z.F., Qi, H.F., Li, J.F., Wang, Y.L., Harding, J., Tu, X., Wang, A.Q., Yan, J.H., Li, X.D., 2021. Direct ammonia synthesis from the air via gliding arc plasma integrated with single atom electrocatalysis. *Appl. Catal., B* 299, 120667.
- Zeldovich, Y. B., 1946. The oxidation of nitrogen in combustion and explosions. *J. Acta Physicochimica* 21, 577.
- Zhou, D., Zhou, R., Zhou, R., Liu, B., Zhang, T., Xian, Y., Cullen, P.J., Lu, X., Ostrikov, K., 2021. Sustainable ammonia production by non-thermal plasmas: status, mechanisms, and opportunities. *Chem. Eng. J.* 421, 129544.